# Mid-infrared laser spectroscopy using a tunable gain-switched $Cr^{2+}$: ZnSe laser

M. Evers, D. Welford, D. Manstein, R. Birngruber

**Absorption spectroscopy in the mid-infrared (mid-IR) is mostly done by Fourier transform infrared (FT-IR) spectroscopy using wide bandwidth light sources [1]. To reduce artifacts and to have the advantage of spatial resolution we built a narrow bandwidth high resolution mid-infrared laser spectroscope using a tunable laser. The broad gain band of the chromium-doped zinc selenide/sulfide laser allows a spectral coverage from 2200nm to 2850nm, wide enough to see typical vibration bands of biological macro-molecules. This provides a unique opportunity to investigate wavelength dependent absorptions of numerous chemical and biological materials.**

**Since the laser should be used for spectroscopic applications, an accurate wavelength calibration was performed. It was also ensured that the optical elements meet the requirements for the use in the mid-IR spectrum and that the results are not distorted by absorption of other substances or by interference.**

## I. Introduction

Infrared spectroscopy is one of the most common spectroscopic techniques used by organic and inorganic chemists [1]. Organic molecules have a large number of strong vibronic absorption lines within the near- and mid-IR spectral range that are characteristic of their structure. Infrared absorption spectroscopy can reveal the structures of covalently bonded chemical compounds exploiting the fact that molecules have a "molecular absorption fingerprint" [2].

The IR spectrum of a molecule is exerted when the IR radiation hits the sample. The molecules absorb the energy and respond by vibrating when the frequency of the light is the same as the vibrational frequency of a bond. Because of this fact, the technique works almost exclusively on molecules with covalent bonds. While changing the wavelength the measurement of the transmitted light exposes how much energy was absorbed at each wavelength. Alternatively, FT-IR spectroscopy is using the whole wavelength range instead of measuring every single wavelength and thus has an advantage of better sensitivity when used in conjunction with broad bond light sources. However, it often produces artifacts and has low spatial resolution [3].

Michael Evers, Medizinische Ingenieurwissenschaft, University of Luebeck; the work has been carried out at the Wellman Center for Photomedicine, Department of Dermatology, Massachusetts General Hospital, Harvard Medical School, Boston, MA, USA (telephone: +1-617-710-3193, e-mail: mevers@partners.org, michaelevers@gmx.net)

David Welford, Ph.D., Endeavour Laser Technologies Inc., Hathorne, MA, USA (telephone: +1-978-764-8787, e-mail: welford@endeavourlaser.com)

Dieter Manstein, M.D., Ph.D., Wellman Center for Photomedicine, Department of Dermatology, Massachusetts General Hospital, Harvard Medical School, Boston, MA, USA (telephone: +1-617-726-4893, e-mail: dmanstein@partners.org)

Prof. Dr. phil. nat. Dr. med. habil. Reginald Birngruber, Institute for Biomedical Optics, University of Luebeck, Germany (email: bgb@bmo.uni-luebeck.de)

In 2010, the fully tunable high power Cr2+: ZnSe laser system within the mid-IR wavelength range of 2250 nm to 2850 nm has become commercially available as a potential source for IR laser spectroscopy. The combination of available pump sources like the Tm fiber laser and the continuous wavelength tunability of this new laser source makes it an exclusive tool for research and offers a large number of possibilities for sensing, including non-invasive medical diagnostic applications, and high-resolution molecular spectroscopy. Furthermore, the tunable laser system may provide the option to perform a combination of spectroscopy and medical treatment in a single device. The narrow bandwidth and the broad tunability which cannot be found at other common devices are ideal for spectroscopic applications, whereas the high output power and the possibility to work at room temperature are essential for clinical use. Another advantage of such a system is that it has the potential of choosing a gain switched and a CW operation mode [4].

The fact that the wavelength is freely tunable within a relatively wide range of the near to the mid-infrared spectrum offers exclusive opportunities to find absorbent materials which could be used as a target for medical treatment.

## II. Material and Methods

### A. Tunable Mid-Infrared Laser System

The tunable Cr2+: ZnSe is a class IV laser system with two independent output channels. One is a high power CW and the other a high energy gain-switched laser (Model CW HTPTL-GS HETL-Integrated, IPG Photonics Corporation, Birmingham, AL, USA). The channels are based on chromium doped zinc selenide/ sulfide gain media and are optically pumped by a CW 40 W Tm-fiber laser operating at 1908 nm (Model TLR-40-1908, IPG Photonics Corporation, Birmingham, AL, USA). The CW laser emits at a central wavelength of 2600 nm and is tunable from 2400 nm to 2800 nm with up to 8.8 W power and a linewidth below 5 nm. The pulsed laser has its central wavelength at 2550 nm and is tunable from 2250 nm to 2850 nm with up to 2.8 mJ energy per pulse at 100 Hz to 1000 Hz repetition rate. When the laser system is in pulse mode, the laser is secondarily pumped by a Q-switched Ho: YAG laser that emits at 2100 nm, which makes pulse duration of 3 ns ± 0.5 ns with 1.5 nm linewidth possible.

While operating, the laser system is cooled by a water cooling system and purged with nitrogen. An illustration of the laser system is shown in Fig.1. The enclosure is also purged with nitrogen because water vapor within the air leads to strong absorption.

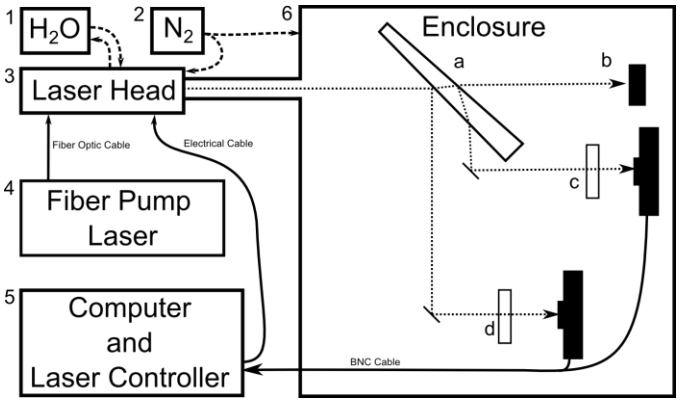


Fig. 1 The $Cr^{2+}$: ZnSe tunable laser system consisting of (1) water cooling system (2) nitrogen purge gas, (3) CW-HTPTL-GS-HETL laser head unit, (4) TLR-40-1908 TM-fiber pump laser unit and Arduino Uno microcontroller board, (5) computer with SMC View Software and laser controller unit, (6) Enclosure with (a) 3° $CaF_2$ window wedge, (b) a beam block, (c) reference arm and (d) sample arm with a silver coated mirror, a cuvette/gas cell and a low power thermal sensor.

Nitrogen was chosen as a purge gas because of its homonuclear diatomic structure which does not absorb in the mid-infrared range [3].

Fig. 2 shows the effect of the purge gas while taking a laser output power curve. For this laser output power measurement, a 100 mm gas cell was either filled with ambient air, nitrogen or water saturated nitrogen and was placed between the laser output and a low power thermal sensor head which was connected to a laser power and energy meter (Vega, Ophir Optronics Ltd., Jerusalem, Israel). Even though there was a pathway of 0.7 mm between the thermal sensor and the gas cell which was filled by ambient air due to the construction of the sensor, the effect of the purge gas is clearly distinguishable. From 2614 nm to 2632 nm four strong absorption peaks exist in air which are even stronger for nitrogen gas saturated with water vapor but much less pronounced for the pure purge gas.

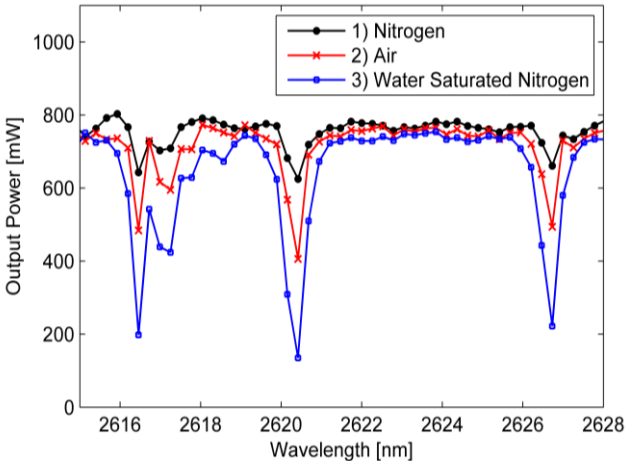


Fig. 2 Power curves show wavelength-dependent output power of the tunable laser at 100% of the maximum pump power at 500 Hz at pulsed mode while the laser beam goes through a 100 mm gas cell filled with nitrogen, air and nitrogen saturated with water vapor. The small unpurged gap between the gas cell and the thermal sensor is responsible for the dips in the first graph.

The APT User 1.0.22 software (Thorlabs, Newton, NJ, USA) controls switching from pulsed to CW operation by changing the position of a mirror which is mounted on a rotation stage and delivers the pump laser light from the Tm-fiber laser source.

The actual spectroscope consists of a wedge, a sample and a reference arm. The wedge is a 3° calcium fluoride ($CaF_2$) window which separates the laser output beam into two reflectance paths and one transmission path (Fig.1). The refractive index in this spectral range is about 1.42 which leads to a reflectance of about 3%. Most of the laser energy is transmitted by the wedge and goes into a beam block. The reflected beams have only 3% of the original energy to prevent overheating of the sample and the formation of cavitation bubbles. Changing the window wedge material from $CaF_2$ to a material with a higher refractive index e.g. Arsenic trisulfide leads to higher reflectance and energy in the sample and reference arm. The sample and the reference arm have the same path length and consist of identical optical elements like a silver coated mirror, a cuvette for near to mid-IR use (infrasil®) and a low power thermal sensor.

### *B. Wavelength Calibration of the Tunable Laser System*

Since the selected laser is widely tunable in the mid-IR wavelength range, the wavelength reading has to be calibrated. The laser wavelength for this system is tuned by a stepper motor, which rotates a diffraction grating within a limited angle range. Each wavelength corresponds to a specific stepper motor position, calculated with the following equation:

$$\frac{\lambda}{nm} = \frac{10^6}{A2}\left(sin(A0) + sin\left(A1 + atan\left(\frac{x}{mm} * \frac{1}{38}\right)\right)\right) \quad (1)$$

$A0 = 0.22213 \quad A1 = 0.55953 \quad A2 = 347.45573$

for the pulsed regime of operation and for CW as follows:

$A0 = 0.12751 \quad A1 = 0.58241 \quad A2 = 327.1037$

where $\lambda$ is the output wavelength measured in [nm] and $x$ is the absolute displacement of the stepper motor measured in [mm] according to the factory calibration.

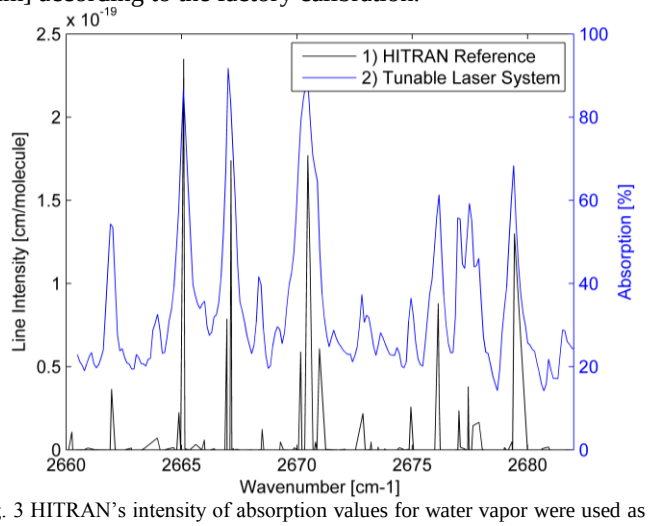


Fig. 3 HITRAN's intensity of absorption values for water vapor were used as a reference. For the pulse-mode of the tunable laser system the measured absorption values had to be shifted of about 10 nm to the left to match with the reference values.

To verify this calibration, the current edition of the high-resolution transmission molecular absorption database (HITRAN 2008) was used.

For the calibration measurements, a 100 mm gas cell was filled with the non-absorbing purge gas nitrogen and placed between the laser output and the low power thermal sensor. Another measurement was done with water saturated nitrogen. For high resolution reasons the stepper motor step size was set to 5 µm which leads to a resolution of 0.28 nm. Even higher resolution can be achieved, by setting the stepper motor to its minimal step size of 0.15 µm which is equivalent to a 12.6 pm resolution. The first measurement was done as a reference so that the absorption of water vapor could be determined. For visual comparison the experimental and the reference data were plotted in one graph. The measured values were shifted until the absorption peaks matched with the HITRAN data (Fig. 3). Afterwards the peaks were compared as seen in Table I.

TABLE I
DIFFERENCE BETWEEN REFERENCE AND EXPERIMENTAL DATA

| Pulse-Mode | N | Ref. | Exp. | Diff. |
|---|---|---|---|---|
| | 1 | 2531.7 | 2543.2 | 11.5 |
| | 2 | 2536.4 | 2547.7 | 11.4 |
| | 16 | 2693.8 | 2703.7 | 9.9 |
| | 17 | 2695.9 | 2705.7 | 9.8 |
| | 32 | 2803.7 | 2812.9 | 9.2 |
| | 33 | 2804.5 | 2813.6 | 9.1 |
| CW-Mode | | | | |
| | 1 | 2550.4 | 2550.9 | 0.5 |
| | 2 | 2552.0 | 2552.7 | 0.7 |
| | 11 | 2692.0 | 2693.8 | 1.8 |
| | 12 | 2694.2 | 2695.8 | 1.6 |
| | 23 | 2755.3 | 2756.1 | 0.8 |
| | 24 | 2762.0 | 2762.7 | 0.7 |

33 peaks from 2531 nm to 2804 nm were compared for the pulse-mode with differences of up to 11.5 nm and 24 peaks from 2551 nm to 2762 nm for the CW-mode with up to 1.8 nm between the measured and the reference data. Because of the deviation from the factory to the reference values, a more accurate fitting curve was generated (Fig. 4). This was done by a non-linear least square fit which calculates new values for the free variables A0, A1 and A2 of equation (1).

$$\min_x \| F(x, x_s) - y_r \|_2^2 = \min_x \sum_i^N \left( F(x, x_{s_i}) - y_{r_i} \right)^2 \qquad (2)$$

where $x_s$ is the stepper motor position, $y_r$ is the wavelength reference data, $N$ is the amount of compared peaks, $x$ is the vector of the free variables A0, A1 and A2 and $F$ is Eq. (1).
The free variables of the new fitting curve for the pulse-mode are: $A0 = 0.1835$ $A1 = 0.5755$ $A2 = 338.796$ and $A0 = 0.0285$ $A1 = 0.6434$ $A2 = 304.7349$ for the CW-mode. Fig. 4 shows a noticeable difference between the factory fitting and the new fitting for the pulse-mode whereas there is little difference between the two fittings for CW-mode.

### C. Interference

Most spectroscopes are using cuvettes and gas cells to study liquid and gaseous samples in the IR light [5]. These cuvettes and gas cells have to be transparent in this spectral range to allow measurements. Therefore fused quartz glass (infrasil®) was chosen with a useable range from 220 nm to 3800 nm. The advantage of these cuvettes and gas cells is their high purity and wide spectral range of use but they are relatively expensive and fragile compared to plastic cuvettes and gas cells.

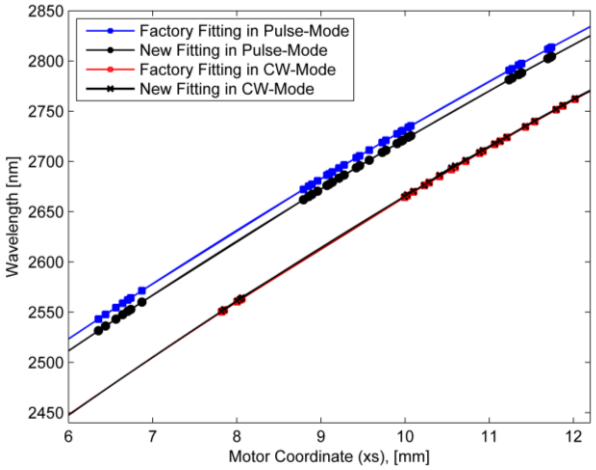


Fig. 4 The wavelength of the factory fitting curve for the pulse and CW-mode were calculated by given values for the free variables A0, A1 and A2 in (1). With the HITRAN reference data new and more accurate values for the free variables of (1) were found. There is a difference of up to 11.5 nm between the calculated and the reference wavelengths for pulse-mode and up to 1.8 nm for CW-mode.

A fused silica cuvette placed in the beam pathway causes a noticeable change in amplitude and frequency of the laser output power as seen in Fig. 5. The Fourier transform of this fringe-pattern is the reciprocal of $\Delta\lambda$, which is the distance between two peaks of the pattern, described by the following equation:

$$\Delta\lambda = \frac{\lambda^2}{2 n_\lambda d * \cos\theta} \qquad (3)$$

For this measurement the thickness $d$ of the used cuvette glass was 1.25 mm and at a wavelength $\lambda$ of 2400 nm the refractive index $n_\lambda$ is 1.432. The cuvette was nearly perpendicular ($\theta$ = 4°) to the laser beam which leads to a value of 1.614 nm for $\Delta\lambda$. The reciprocal of the Fourier transform shown in Fig. 6 has a result for $\Delta\lambda$ which is very close to that. This provides evidence that the fringes are not caused by absorption of the cuvette itself, but are caused by reflectance which leads to constructive and destructive interference.

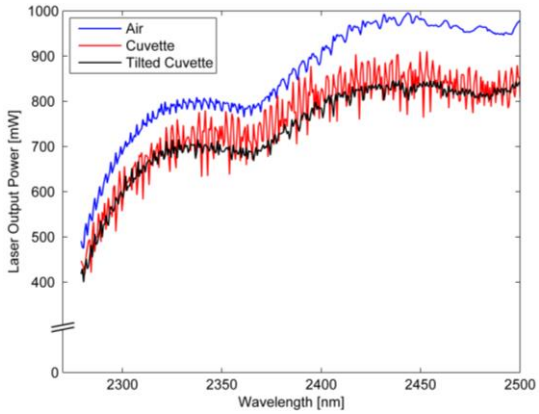


Fig. 5 The measured laser output power of the pulsed laser after a 90 mm pathway of air with and without an empty cuvette. The cuvette causes reflectance and constructive and destructive interference. To reduce the interference the cuvette was heavily tilted.

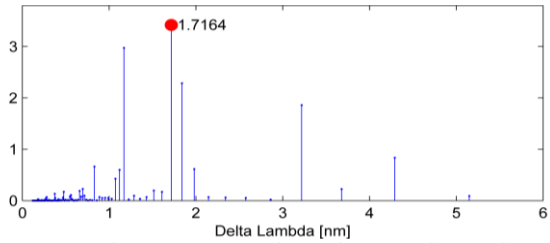


Fig. 6 The result of the Fourier transform of the interference fringe is the reciprocal of $\Delta\lambda$.The highest peak is at 1.7164 nm which is close to the result of (3) and confirms the theory that the interference origin are reflections at the 1.25 mm thick cuvette glass wall.

## III. Results and Discussion

### A. Absorption of Air

While doing experiments in the ambient air at specific wavelengths the output power of the laser system was lower than expected and buzzing sounds were noticed in pulsed operation mode. Water vapor molecules have many vibrational bands in the mid-IR range and absorb most of the output laser energy at numerous wavelengths. This leads to a fast thermal expansion which generated the buzzing sound and lowered the transmitted energy. In CW operation there are no buzzing sounds and the energy loss is much less pronounced based on the wider linewidth. Figure 7 shows an absorption spectrum in pulse mode where the laser beam went through 73.5 cm of ambient air. The water vapor absorption starts at around 2550 nm and is the reason for most of the absorption peaks with up to 98 % absorption.

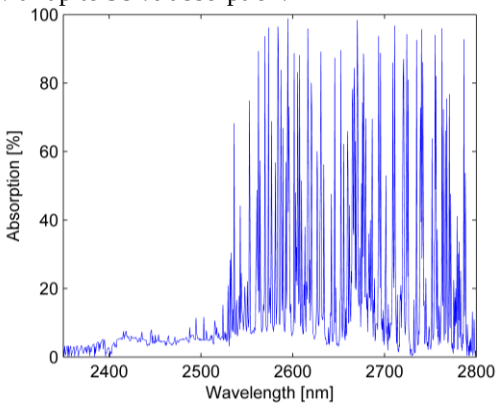


Fig. 7 Absorption of air in pulse-mode at 500 Hz. The pathway between laser output and thermal sensor is 73.5 cm. The main absorber in this spectrum is water vapor.

### B. Absorption of Biological Substances

The absorption property of water has been studied in detail by many research groups [6], whereas the mid-IR absorption of human fat was analyzed by only a few researchers [8]. Therefore we investigated human fat and one of its components, squalene which can be found in high concentrations in human fat and is one of the major components of skin surface lipids. The absorption spectra shown in Fig. 8 were measured in a 1 mm cuvette for each sample and are close to those found in literature. At 2306 nm the absorption of human fat has a local maximum and is even higher than the water absorption. This finding has been reported by Dieter Manstein in 2006 [7]. At about 2650 nm the difference between the absorption of water and human fat has its maximum. This circumstance could have a clinical relevance for example for optical applications in the human body which require strong water and low fat absorption.

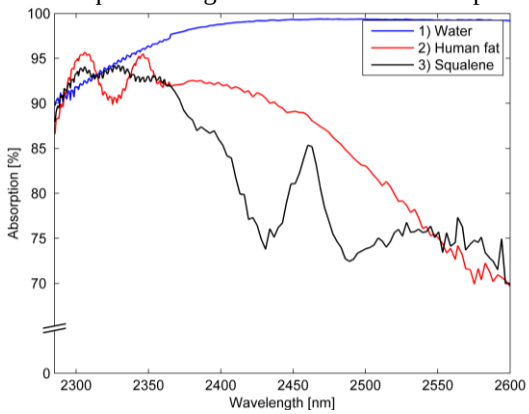


Fig. 8 Absorption spectra of biological chromophores like water, human fat and squalene measured in a 1 mm cuvette in pulse mode (500 Hz).

## IV. Conclusions and Future Work

For future medical and spectroscopic applications with this experimental setup the user has to keep in mind the strong water vapor absorption at specific wavelengths. The path length of the IR laser light through normal atmosphere should therefore be kept as small as possible and the use of a purge gas is expedient. Water is necessary for the function of many biological systems and processes. However, the absorption of liquid water in some regions of the mid-IR range is extremely high and the light is entirely absorbed when the beam passes through some tens of micrometers [3]. Therefore cuvettes with very small sample volumes should be used. Even with the enclosure purged with dry nitrogen there was still some water vapor absorption left. This can be reduced by a better isolation of the laser and the enclosure. One way to eliminate these absorptions completely is to put the whole setup in a vacuum. However, this would be very costly in terms of labor and money.

In the presented work, error sources like water absorption and interference were corrected, the basic setup of the spectroscope was built and some biological materials were analyzed. In Future, the spectroscope will be completed and upgraded to do spatially resolved spectroscopy and to analyze absorption properties of a tissue phantom made out of gelatin.

## References

[1] C.-P Sherman Hsu, "Infrared spectroscopy", *Handbook of Instrumental Techniques for Analytical Chemistry*, Editor F.A. Settle, New Jersey, 1997, pp. 247-283

[2] "Infrared Spectroscopy", *Online edition for students or organic lab courses at the University of Colorado*, Boulder, 2002, pp.155-164

[3] P. Kosters, "FT-IR spectroscopy of thin biological layers", *PhD thesis*, University of Twente, 2000

[4] M.L.Ha, "Fractional laser ablation of cutaneous tissue using a tunable CW and gain-switched chromium-doped zinc chalcogenide IR laser", *Master's thesis*, University of Luebeck, 2012

[5] F. Siebert and P. Hildebrandt, *Vibrational Spectroscopy in Life Science"*, Wiley-VCH, Weinheim, 2008

[6] G. M. Hale, M. R. Querry, "*Optical constants of water in the 200 nm to 200 µm wavelength region*", Appl. Opt, vol.12, 555-563 (1973).

[7] R.R. Anderson, W. Farinelli, H. Laubach, D. Manstein "Selective Photothermolysis of Lipid-rich tissue: a free electron laser study", Lasers Surg Med. 2006 Dec;38(10): 913-9